Proceedings of the Estonian Academy of Sciences,
2020, **69**, 4, 368–381
https://doi.org/10.3176/proc.2020.4.06
Available online at www.eap.ee/proceedings

COMMUNICATIONS
TECHNOLOGY

Non-linear energy harvesting based power splitting relaying in full-duplex AF and DF relaying networks: system performance analysis

Tran Tin Phu[a], Duc-Van Phan[b], Duy-Hung Ha[c], Tan N. Nguyen[d*], Minh Tran[e], and Miroslav Voznak[c]

[a] Faculty of Electronics Technology, Industrial University of Ho Chi Minh City, Ho Chi Minh City, Vietnam
[b] Faculty of Automobile Technology, Van Lang University, Ho Chi Minh City, Vietnam
[c] Faculty of Electrical Engineering and Computer Science, VSB - Technical University of Ostrava, 17. listopadu 2172/15, Ostrava, Czech Republic
[d] Wireless Communications Research Group, Faculty of Electrical and Electronics Engineering, Ton Duc Thang University, Ho Chi Minh City, Vietnam
[e] Optoelectronics Research Group, Faculty of Electrical and Electronics Engineering, Ton Duc Thang University, Ho Chi Minh City, Vietnam

Received 3 July 2020, accepted 20 september 2020, available online 30 October 2020

Abstract. Wireless power transfer is considered as a novel solution for energy harvesting in wireless communication networks. In this paper, the system performance of the non-linear energy harvesting based power splitting relaying in the full-duplex relaying sensor network is investigated. We considered the system model network with one source, one destination, and one relay node in both the amplify-and-forward and decode-and-forward modes. The closed-form expressions of the system outage (OP) are analysed and derived for verifying system performance. Then, the correctness of the OP closed-form expression is verified by using the Monte Carlo simulation. Furthermore, the influence of the primary system parameters on the system OP is suggested and investigated. The research results indicated that the simulation curves and the analytical curves overlapped, verifying the correctness of the analytical expressions.

Key words: amplify-and-forward, decode-and-forward, outage probability, non-linear energy harvesting, sensors network.

Abbreviations and symbols

AF	Amplify-and-forward
AWGN	Additive white Gaussian noise
DF	Decode-and-forward
EH	Energy harvesting
FD	Full-duplex
IT	Information transformation
NEH	Non-linear energy harvesting
OP	Outage probability
PS	Power splitting
RF	Radiofrequency
RV	Random variable
SINR	Signal to interference noise ratio
SP	Success probability
SWIPT	Simultaneous wireless information and power transfer
ρ	Power splitting factor, $0 < \rho < 1$
η	Energy conversion efficiency, $0 < \eta \leq 1$
P_{th}	Saturation threshold of the rechargeable power
γ_{th}	Threshold of the system
$\Gamma(\bullet)$	Incomplete gamma function
λ_{SR}	Mean of $\lvert h_{SR}\rvert^2$
λ_{RD}	Mean of $\lvert h_{RD}\rvert^2$
Ω_{RR}	Variance of $\lvert h_{RR}\rvert^2$
β	Amplification factor
P_S	Transmit power of the source
T	Total time of processing
ψ	Ratio of energy P_s to variance N_0

* Corresponding author, nguyennhattan@tdtu.edu.vn

1. INTRODUCTION

In comparison with other energy harvesting (EH) methods, such as from the sun, heat, wind, motion, etc., radiofrequency (RF) EH can be considered as a novel solution because energy can transfer through the air without a cable and both energy and information can be carried using the RF signal [1–4]. In wireless communications this technique is a comfortable solution for battery-limited applications or under conditions that are dangerous for operating devices. For this purpose, a novel technique called simultaneous wireless information and power transfer (SWIPT) is proposed based on the fact that the RF signals can transfer information and energy simultaneously. The SWIPT technique can help the energy-constrained nodes harvest energy from other nodes or the surrounding environment and use this energy to transfer information to other nodes [1–10]. Recently SWIPT has attracted significant attention in academia.

In [6] the fundamental tradeoff between the transporting and the information rate is presented and investigated. Improving the efficiency of simultaneous information transmission and energy transferring by using some fundamental tradeoffs in designing wireless multiple-input multiple-output (MIMO) systems is studied in [11]. In [12] the authors investigate a joint beamforming algorithm for a multiuser wireless communication network system and compare these systems with conventional systems. In [13] a multiuser multiple-input single-output broadcast SWIPT system is proposed and analysed.

The interference channel in SWIPT is carefully studied in [14–16]. In [14] a geodesic energy beamforming scheme with channel state information (CSI) is proposed to reduce the feedback overhead in the communication system. A novel approach for realizing SWIPT in a broadband system with orthogonal frequency division multiplexing and transmit beamforming is proposed and investigated in [15]. In [16] the optimal design for SWIPT in downlink multiuser orthogonal frequency division multiplexing systems where the users harvest energy and decode information using the same signals received from a fixed access point is studied.

A cooperative relaying communication network in both amplify-and-forward (AF) and decode-and-forward (DF) modes is considered in [17–19]. In that network an energy-constrained relay node receives the energy from the source node, and the information is transferred from the source node to the destination with the help of a relay. Wireless powered communication and its potential applications and promising research directions are studied in [20–24]. Moreover, in [25] the theoretical symbol error probability (SEP) of a cooperative relaying system network is derived. In [26] a novel distributed space-time block code (DSTBC) scheme in multihop power line communication (PLC) networks is proposed. In [27] a simple adaptive relaying protocol (ARP) for general relaying system networks is studied. From this review of literature, we can state that the research direction in SWIPT is extremely hot and needs to be developed more and more.

In SWIPT the rectenna is considered as a critical component of the far-field RF harvesting circuits because of the conversion of the input RF signal to DC voltage by the antenna and the rectifier. The non-linearity of harvested power as a function of input power is also corroborated by the fact that the conversion efficiency in the literature on microwave circuits is always referenced to a specific level of input power [28–30].

To the best of our knowledge, there are very few recent SWIPT researches that study non-linear RF harvesting models. In this paper the system performance analysis of non-linear energy harvesting (NEH) based power splitting (PS) relaying in full-duplex (FD) relaying networks is proposed and investigated. In this research we considered the system network with one source (S) and one destination (D) node, which communicate by helping the intermediate relay (R) node in both AF and DF modes. The closed-form expressions of the system outage probability (OP) are analysed and derived for both AF and DF modes. Then, the correctness of the analytical OP is verified by using the Monte Carlo simulation. Furthermore, the influence of the primary system parameters on the system OP is investigated. The research results indicated that the simulation curves and the analytical curves overlapped, verifying the correctness of the analytical expressions. Here are the main contributions of this research:

- NEH based PS relaying in the FD relaying sensor network is presented.
- The closed form of the system OP in both the AF and the DF mode is derived.
- The Monte Carlo simulation is conducted to verify the correctness of the results, and the effect of the main system parameters on the system OP is analysed.

The structure of the rest of this paper is as follows. Section 2 presents the system model, the energy harvesting, and information transmission phases. Section 3 presents the OP analysis for deriving the closed form of the system OP. Section 4 proposes some numerical results and discussions. Finally, some conclusions are drawn in Section 5.

2. SYSTEM MODEL

The NEH based PS relaying in the FD relaying sensor network is proposed in Fig. 1. In addition, the loopback interference is considered at R. In this system model, all links are Rayleigh block fading channels.

The EH and information transformation (IT) for the proposed model system are illustrated in Fig. 2. The time of information transmission and energy transferring is denoted as T. In the interval T, the relay R harvests energy ρP_s from the source node S, and the source uses the energy $(1-\rho)P_s$ for information transmission to the relay R and the destination D (here ρ is the power splitting factor) [31–34].

2.1. Non-linear energy harvesting phase

In the EH phase, the received signal at the relay can be given as

$$y_r = \sqrt{\rho P_s} h_{SR} x_s + n_r, \tag{1}$$

where x_s is the transmit signal at the source and $\mathrm{E}\left\{\left|x_s\right|^2\right\}=1$, $\mathrm{E}\{\bullet\}$ is the expectation operator, h_{SR} is the channel coefficient, n_r is the zero-mean additive white Gaussian noise (AWGN) with variance N_0.

In most literature, the total harvested energy at the relay is formulated as a linear model [31–34]. In this paper, the non-linear transformation model proposed in reference [35–37] is used. The average transmit power at the relay can be obtained as

$$P_r = \begin{cases} \eta\rho P_s \left|h_{SR}\right|^2, P_s \left|h_{SR}\right|^2 \le P_{th} \\ \eta\rho P_{th}, \qquad P_s \left|h_{SR}\right|^2 > P_{th} \end{cases}, \tag{2}$$

where P_{th} is the saturation threshold of the rechargeable power of the hardware circuit.

2.2. Information transmission phase

The received signal at the relay R in the information transmission phase is

$$y_r = \sqrt{(1-\rho)P_s} h_{SR} x_s + \sqrt{P_r} h_{RR} x_r + n_r, \tag{3}$$

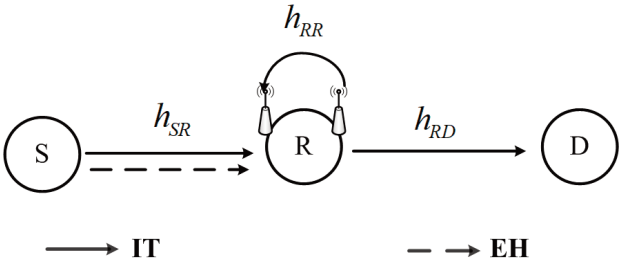

Fig. 1. System model. S denotes source, D is the destination and R stands for relay; h_{SR} and h_{RD} are channel coefficients, and h_{RR} is the loopback interference coefficient.

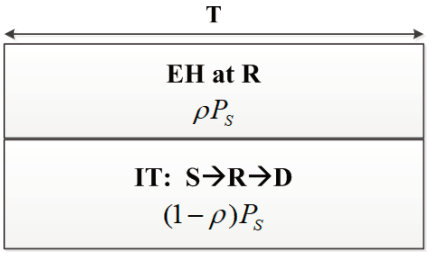

Fig. 2. Energy harvesting and information processing.

where x_r is the loopback interference and $\mathrm{E}\left\{\left|x_r\right|^2\right\}=1$, h_{RR} is the loopback interference channel coefficient. In this phase, the received signal at the destination can be formulated as

$$y_d = \sqrt{P_r}h_{RD}x_r + n_d\,, \tag{4}$$

where h_{RD} is the channel coefficient and n_d is the zero mean AWGN with variance N_0.

2.2.1. AF mode

In the AF protocol, the relay amplification factor β is set as

$$\beta = \frac{x_r}{y_r} = \sqrt{\frac{1}{(1-\rho)\left|h_{SR}\right|^2 P_s + \left|h_{RR}\right|^2 P_r + N_0}}\,. \tag{5}$$

Please note that for convenience in this analysis the residual self-interference at the relay nodes is modelled as AWGN with zero mean and variance Ω_{RR} [33,38].

Hence, the amplification factor can be rewritten as

$$\beta = \sqrt{\frac{1}{(1-\rho)\left|h_{SR}\right|^2 P_s + \Omega_{RR}P_r + N_0}}\,. \tag{6}$$

By substituting (5) into (4) and then combining with (3), we have that

$$\begin{aligned} y_d &= \sqrt{P_r}h_{RD}\beta y_r + n_d = \sqrt{P_r}h_{RD}\beta\left[\sqrt{(1-\rho)P_s}h_{SR}x_s + \sqrt{P_r}h_{RR}x_r + n_r\right] + n_d \\ &= \underbrace{\sqrt{P_r}h_{RD}\beta\sqrt{(1-\rho)P_s}h_{SR}x_s}_{signal} + \underbrace{\sqrt{P_r}h_{RD}\beta\sqrt{P_r}h_{RR}x_r}_{\mathrm{int}\,erference-noise} + \underbrace{\sqrt{P_r}h_{RD}\beta n_r + n_d}_{noise}\,. \end{aligned} \tag{7}$$

The end to end signal to the interference noise ratio (SINR) from (7) can be obtained as

$$\begin{aligned} SINR_{AF} &= \frac{\mathrm{E}\left\{\left|signal\right|^2\right\}}{\mathrm{E}\left\{\left|interference-noise\right|^2\right\} + \mathrm{E}\left\{\left|noise\right|^2\right\}} \\ &= \frac{(1-\rho)P_rP_s\left|h_{SR}\right|^2\left|h_{RD}\right|^2\beta^2}{P_r^2\left|h_{RD}\right|^2\Omega_{RR}\beta^2 + P_r\left|h_{RD}\right|^2\beta^2N_0 + N_0} \\ &= \frac{(1-\rho)P_rP_s\left|h_{SR}\right|^2\left|h_{RD}\right|^2}{P_r^2\left|h_{RD}\right|^2\Omega_{RR} + P_r\left|h_{RD}\right|^2N_0 + \frac{N_0}{\beta^2}}. \end{aligned} \tag{8}$$

After doing some algebra, equation (8) can be reformulated as

$$SINR_{AF} \approx \frac{(1-\rho)P_s\left|h_{SR}\right|^2\left|h_{RD}\right|^2}{P_r\left|h_{RD}\right|^2\Omega_{RR} + \frac{(1-\rho)\left|h_{SR}\right|^2P_sN_0}{P_r} + N_0\Omega_{RR}}\,. \tag{9}$$

2.2.2. DF mode

In the DF mode, the SINR at the relay R from (3) can be given as

$$SINR_R = \frac{(1-\rho)P_s |h_{SR}|^2}{P_r \Omega_{RR} + N_0}. \tag{10}$$

From (4), the SINR at the destination D can be expressed as

$$SINR_D = \frac{P_r |h_{RD}|^2}{N_0}. \tag{11}$$

3. SYSTEM PERFORMANCE

3.1. AF mode

In the AF mode the OP can be defined as

$$OP_{AF} = 1 - SP_{AF},$$

where SP_{AF} is the success probability (SP), which can be given as follows:

$$SP_{AF} = \Pr\left(SINR_{AF} > \gamma_{th}\right) = \Pr\left(\frac{(1-\rho)P_s |h_{SR}|^2 |h_{RD}|^2}{P_r |h_{RD}|^2 \Omega_{RR} + \frac{(1-\rho)|h_{SR}|^2 P_s N_0}{P_r} + N_0 \Omega_{RR}} > \gamma_{th} \right), \tag{12}$$

where γ_{th} is the threshold of the system.

By substituting (3) into (12), equation (12) can be rewritten as

$$SP_{AF} = \Pr\left(\frac{(1-\rho)P_s |h_{SR}|^2 |h_{RD}|^2}{\eta\rho P_s |h_{SR}|^2 |h_{RD}|^2 \Omega_{RR} + \frac{(1-\rho)N_0}{\eta\rho} + N_0 \Omega_{RR}} > \gamma_{th}, P_s |h_{SR}|^2 \le P_{th} \right)$$

$$+ \Pr\left(\frac{(1-\rho)P_s |h_{SR}|^2 |h_{RD}|^2}{\eta\rho P_{th} |h_{RD}|^2 \Omega_{RR} + \frac{(1-\rho)|h_{SR}|^2 P_s N_0}{\eta\rho P_{th}} + N_0 \Omega_{RR}} > \gamma_{th}, P_s |h_{SR}|^2 > P_{th} \right) = P_1 + P_2, \tag{13}$$

where

$$P_1 = \Pr\left(\frac{(1-\rho)P_s |h_{SR}|^2 |h_{RD}|^2}{\eta\rho P_s |h_{SR}|^2 |h_{RD}|^2 \Omega_{RR} + \frac{(1-\rho)N_0}{\eta\rho} + N_0 \Omega_{RR}} > \gamma_{th}, P_s |h_{SR}|^2 \le P_{th} \right). \tag{14}$$

We denote $X = |h_{SR}|^2$, $Y = |h_{RD}|^2$ and $a_1 = \eta\rho(1-\rho)P_s, b_1 = \eta^2\rho^2 P_s \Omega_{RR}$, $c_1 = (1-\rho)N_0 + \eta\rho N_0 \Omega_{RR}$, $d = \dfrac{P_{th}}{P_s}$; so equation (14) can be reformulated as

$$P_1 = \Pr\left(\frac{a_1 XY}{b_1 XY + c_1} > \gamma_{th}, X \le d\right) = \int_0^d \underbrace{\Pr\left(\frac{a_1 xY}{b_1 xY + c_1} > \gamma_{th}\right)}_{\Phi(x)} f_x(x)dx \,. \tag{15}$$

Consider

$$\Phi(x) = \Pr\left(\frac{a_1 xY}{b_1 xY + c_1} > \gamma_{th}\right) = \Pr\left[xY\left(a_1 - \gamma_{th}b_1\right) > \gamma_{th}c_1\right]$$

$$= \begin{cases} \Pr\left[Y > \dfrac{\gamma_{th}c_1}{x\left(a_1 - \gamma_{th}b_1\right)}\right], a_1 > \gamma_{th}b_1 \\ 0 \qquad\qquad\qquad\qquad , a_1 \le \gamma_{th}b_1 \end{cases} = \begin{cases} \exp\left[-\dfrac{\lambda_{RD}\gamma_{th}c_1}{x\left(a_1 - \gamma_{th}b_1\right)}\right], a_1 > \gamma_{th}b_1 \\ 0 \qquad\qquad\qquad\qquad , a_1 \le \gamma_{th}b_1 \end{cases}, \tag{16}$$

where λ_{RD} is the mean value of the random variable (RV) $|h_{RD}|^2$.

If we choose the condition of the threshold $a_1 > \gamma_{th}b_1 \leftrightarrow \gamma_{th} < \dfrac{a_1}{b_1}$ then by substituting (16) into (15) P_1 can be obtained as follows:

$$P_1 = \lambda_{SR}\int_0^d \exp\left[-\frac{\lambda_{RD}\gamma_{th}c_1}{x\left(a_1 - \gamma_{th}b_1\right)}\right] \times \exp\left(-\lambda_{SR}x\right)dx, \tag{17}$$

where λ_{SR} is the mean value of the RV $|h_{SR}|^2$.

Apply Taylor series as follows:

$$\exp\left(-\lambda_{SR}x\right) = \sum_{k=0}^{\infty}\frac{\left(-\lambda_{SR}x\right)^k}{k!} = \sum_{k=0}^{\infty}\frac{(-1)^k\left(\lambda_{SR}\right)^k}{k!}x^k \,. \tag{18}$$

Substituting (18) into (17), we have

$$P_1 = \sum_{k=0}^{\infty}\frac{(-1)^k\left(\lambda_{SR}\right)^{k+1}}{k!}\int_0^d \exp\left[-\frac{x^{-1}\lambda_{RD}\gamma_{th}c_1}{\left(a_1 - \gamma_{th}b_1\right)}\right]x^k dx \,. \tag{19}$$

By changing variable $t = \dfrac{1}{x}$, equation (19) can be rewritten as

$$P_1 = \sum_{k=0}^{\infty}\frac{(-1)^k\left(\lambda_{SR}\right)^{k+1}}{k!}\int_{1/d}^{\infty} \exp\left[-\frac{t\lambda_{RD}\gamma_{th}c_1}{\left(a_1 - \gamma_{th}b_1\right)}\right] \times t^{-k-2}dt \,. \tag{20}$$

By applying equation (3.381,3) from the table of integrals [38], equation (20) can finally be obtained as

$$P_1 = \sum_{k=0}^{\infty}\frac{(-1)^k\left(\lambda_{SR}\right)^{k+1}}{k!} \times \left[\frac{\lambda_{RD}\gamma_{th}c_1}{\left(a_1 - \gamma_{th}b_1\right)}\right]^{k+1} \times \Gamma\left(-k-1, \frac{\lambda_{RD}\gamma_{th}c_1}{\left(a_1 - \gamma_{th}b_1\right)d}\right), \tag{21}$$

where $\Gamma(\alpha, x) = \int_x^{\infty} e^{-t}t^{\alpha-1}dt$ is an incomplete gamma function.

Now we will consider P_2:

$$P_2 = \Pr\left(\begin{array}{l} \dfrac{(1-\rho)P_s |h_{SR}|^2 |h_{RD}|^2}{\eta\rho P_{th} |h_{RD}|^2 \Omega_{RR} + \dfrac{(1-\rho)|h_{SR}|^2 P_s N_0}{\eta\rho P_{th}} + N_0\Omega_{RR}} \\ > \gamma_{th}, P_s |h_{SR}|^2 > P_{th} \end{array} \right). \tag{22}$$

We denote that $a_2 = \eta\rho(1-\rho)P_sP_{th}$, $b_2 = \eta^2\rho^2P_{th}^2\Omega_{RR}$, $c_2 = (1-\rho)P_sN_0$, $e_2 = \eta\rho P_{th}N_0\Omega_{RR}$. Hence, equation (22) can be reformulated as

$$P_2 = \Pr\left(\frac{a_2XY}{b_2Y + c_2X + e_2} > \gamma_{th}, X > d \right) = \int_d^\infty \underbrace{\Pr\left(\frac{a_2xY}{b_2Y + c_2X + e_2} > \gamma_{th} \right)}_{\Xi(x)} f_x(x)dx. \tag{23}$$

Consider

$$\begin{aligned} \Xi(x) &= \Pr\left(\frac{a_2xY}{b_2Y + c_2x + e_2} > \gamma_{th} \right) = \Pr\left[Y(a_2x - \gamma_{th}b_2) > \gamma_{th}c_2x + \gamma_{th}e_2 \right] \\ &= \begin{cases} \Pr\left[Y > \dfrac{\gamma_{th}c_2x + \gamma_{th}e_2}{a_2x - \gamma_{th}b_2} \right], x > \dfrac{\gamma_{th}b_2}{a_2} \\ 0 \qquad\qquad\qquad\qquad , x \le \dfrac{\gamma_{th}b_2}{a_2} \end{cases} = \begin{cases} \exp\left[-\dfrac{\lambda_{RD}(\gamma_{th}c_2x + \gamma_{th}e_2)}{a_2x - \gamma_{th}b_2} \right], x > \dfrac{\gamma_{th}b_2}{a_2} \\ 0 \qquad\qquad\qquad\qquad\qquad , x \le \dfrac{\gamma_{th}b_2}{a_2} \end{cases}. \end{aligned} \tag{24}$$

By substituting (24) into (23), P_2 can be obtained as

$$\begin{aligned} P_2 &= \lambda_{SR} \int_{\max\left(d, \frac{\gamma_{th}b_2}{a_2}\right)}^\infty \exp\left[-\frac{\lambda_{RD}(\gamma_{th}c_2x + \gamma_{th}e_2)}{a_2x - \gamma_{th}b_2} \right] \times \exp(-\lambda_{SR}x)dx \\ &= \lambda_{SR} \int_\Delta^\infty \exp\left[-\frac{\lambda_{RD}(\gamma_{th}c_2x + \gamma_{th}e_2)}{a_2x - \gamma_{th}b_2} \right] \times \exp(-\lambda_{SR}x)dx, \end{aligned} \tag{25}$$

where $\Delta = \max\left(d, \dfrac{\gamma_{th}b_2}{a_2} \right)$.

The changing variable $y = a_2x - \gamma_{th}b_2 \to x = \dfrac{y + \gamma_{th}b_2}{a_2}$. Therefore, equation (25) can be rewritten as

$$P_2 = \lambda_{SR} \int_\Upsilon^\infty \exp\left[-\frac{\lambda_{RD}\left(\gamma_{th}c_2\left[\dfrac{y + \gamma_{th}b_2}{a_2} \right] + \gamma_{th}e_2 \right)}{y} \right] \times \exp\left(-\lambda_{SR}\left[\frac{y + \gamma_{th}b_2}{a_2} \right] \right) dx$$

$$= \frac{\lambda_{SR}}{a_2} \times \exp\left[-\frac{\lambda_{RD}\gamma_{th}c_2}{a_2} - \frac{\lambda_{SR}\gamma_{th}b_2}{a_2} \right] \times \int_\Upsilon^\infty \exp\left(-\frac{\dfrac{\lambda_{RD}\gamma_{th}^2b_2c_2}{a_2} + \gamma_{th}e_2}{y} \right) \times \exp\left(-\frac{\lambda_{SR}y}{a_2} \right) dy, \tag{26}$$

where $\Upsilon = \dfrac{a_2\Delta}{\gamma_{th}b_2}$.

Then we apply the Taylor series as follows:

$$\exp\left(-\frac{\dfrac{\lambda_{RD}\gamma_{th}^2 b_2 c_2}{a_2}+\gamma_{th}e_2}{y}\right)=\sum_{m=0}^{\infty}\frac{\left(-\dfrac{\dfrac{\lambda_{RD}\gamma_{th}^2 b_2 c_2}{a_2}+\gamma_{th}e_2}{y}\right)^m}{m!}=\sum_{m=0}^{\infty}\frac{(-1)^m\left(\dfrac{\lambda_{RD}\gamma_{th}^2 b_2 c_2}{a_2}+\gamma_{th}e_2\right)^m}{m!}y^{-m}. \tag{27}$$

By substituting (27) and (2)6 and applying equation (3.381,3) from the table of integrals [38], P_2 can finally be expressed as

$$P_2=\exp\left[-\frac{\lambda_{RD}\gamma_{th}c_2}{a_2}-\frac{\lambda_{SR}\gamma_{th}b_2}{a_2}\right]\times\sum_{m=0}^{\infty}\frac{(-1)^m\left(\dfrac{\lambda_{RD}\gamma_{th}^2 b_2 c_2}{a_2}+\gamma_{th}e_2\right)^m}{m!}\times\left(\frac{\lambda_{SR}}{a_2}\right)^{-m+2}\times\Gamma\left(-m+1,\frac{\lambda_{SR}\Upsilon}{a_2}\right). \tag{28}$$

By substituting (21) and (28) into (13), the SP of the system can be obtained as

$$SP_{AF}=\sum_{k=0}^{\infty}\frac{(-1)^k\left(\lambda_{SR}\right)^{k+1}}{k!}\times\left[\frac{\lambda_{RD}\gamma_{th}c_1}{\left(a_1-\gamma_{th}b_1\right)}\right]^{k+1}\times\Gamma\left(-k-1,\frac{\lambda_{RD}\gamma_{th}c_1}{\left(a_1-\gamma_{th}b_1\right)d}\right)+\exp\left[-\frac{\lambda_{RD}\gamma_{th}c_2}{a_2}-\frac{\lambda_{SR}\gamma_{th}b_2}{a_2}\right]$$
$$\times\sum_{m=0}^{\infty}\frac{(-1)^m\left(\dfrac{\lambda_{RD}\gamma_{th}^2 b_2 c_2}{a_2}+\gamma_{th}e_2\right)^m}{m!}\times\left(\frac{\lambda_{SR}}{a_2}\right)^{-m+2}\times\Gamma\left(-m+1,\frac{\lambda_{SR}\Upsilon}{a_2}\right). \tag{29}$$

Finally, the OP of the system in the AF mode can be claimed as

$$OP_{AF}=1-\sum_{k=0}^{\infty}\frac{(-1)^k\left(\lambda_{SR}\right)^{k+1}}{k!}\times\left[\frac{\lambda_{RD}\gamma_{th}c_1}{\left(a_1-\gamma_{th}b_1\right)}\right]^{k+1}\times\Gamma\left(-k-1,\frac{\lambda_{RD}\gamma_{th}c_1}{\left(a_1-\gamma_{th}b_1\right)d}\right)-\exp\left[-\frac{\lambda_{RD}\gamma_{th}c_2}{a_2}-\frac{\lambda_{SR}\gamma_{th}b_2}{a_2}\right]$$
$$\times\sum_{m=0}^{\infty}\frac{(-1)^m\left(\dfrac{\lambda_{RD}\gamma_{th}^2 b_2 c_2}{a_2}+\gamma_{th}e_2\right)^m}{m!}\times\left(\frac{\lambda_{SR}}{a_2}\right)^{-m+2}\times\Gamma\left(-m+1,\frac{\lambda_{SR}\Upsilon}{a_2}\right). \tag{30}$$

3.2. DF mode

From equations (10) and (11), the end to end SINR of the DF mode can be given as

$$SINR_{DF}=\min\left(SINR_R,SINR_D\right)=\min\left[\frac{\left(1-\rho\right)P_s\left|h_{SR}\right|^2}{P_r\Omega_{RR}+N_0},\frac{P_r\left|h_{RD}\right|^2}{N_0}\right]. \tag{31}$$

The SP in the DF mode can be expressed as

$$SP_{DF} = \Pr\left(SINR_{DF} > \gamma_{th}\right) = \Pr\left\{\min\left[\frac{(1-\rho)P_s|h_{SR}|^2}{P_r\Omega_{RR}+N_0}, \frac{P_r|h_{RD}|^2}{N_0}\right] > \gamma_{th}\right\}$$
$$= \Pr\left\{\frac{(1-\rho)P_s|h_{SR}|^2}{P_r\Omega_{RR}+N_0} > \gamma_{th}, \frac{P_r|h_{RD}|^2}{N_0} > \gamma_{th}\right\}. \quad (32)$$

We consider the term of equation (32) by substituting equation (2) and by denoting as above in the AF mode: $X = |h_{SR}|^2, Y = |h_{RD}|^2, d = \frac{P_{th}}{P_s}$.

$$\Pr\left\{\frac{(1-\rho)P_s|h_{SR}|^2}{P_r\Omega_{RR}+N_0} > \gamma_{th}, \frac{P_r|h_{RD}|^2}{N_0} > \gamma_{th}\right\} = \Pr\left\{\frac{(1-\rho)P_sX}{\eta\rho P_sX\Omega_{RR}+N_0} > \gamma_{th}, \frac{\eta\rho P_sXY}{N_0} > \gamma_{th}, X \le d\right\}$$
$$+ \Pr\left\{\frac{(1-\rho)P_sX}{\eta\rho P_{th}\Omega_{RR}+N_0} > \gamma_{th}, \frac{\eta\rho P_{th}Y}{N_0} > \gamma_{th}, X > d\right\} = P_3 + P_4, \quad (33)$$

where

$$P_3 = \Pr\left\{\begin{array}{l}\frac{(1-\rho)P_s|h_{SR}|^2}{\eta\rho P_s|h_{SR}|^2\Omega_{RR}+N_0} > \gamma_{th}, \frac{\eta\rho P_s|h_{SR}|^2|h_{RD}|^2}{N_0} > \gamma_{th}, \\ P_s|h_{SR}|^2 \le P_{th}\end{array}\right\}$$
$$= \Pr\left\{\begin{array}{l}\frac{\eta\rho P_sXY}{N_0} > \gamma_{th}, \left((1-\rho)P_s - \eta\rho P_s\gamma_{th}\Omega_{RR}\right)X > \gamma_{th}N_0, \\ X \le d\end{array}\right\}. \quad (34)$$

In the AF mode we selected the condition $\gamma_{th} < \frac{a_1}{b_1} = \frac{1-\rho}{\eta\rho\Omega_{RR}}$. Hence, the condition $(1-\rho)P_s - \eta\rho P_s\gamma_{th}\Omega_{RR} > 0$ is satisfied.

If $d < \frac{\gamma_{th}N_0}{(1-\rho)P_s - \eta\rho P_s\gamma_{th}\Omega_{RR}} \Leftrightarrow P_{th} < \frac{\gamma_{th}N_0}{(1-\rho) - \eta\rho\gamma_{th}\Omega_{RR}}$,

the inequality $\frac{\gamma_{th}N_0}{(1-\rho)P_s - \eta\rho P_s\gamma_{th}\Omega_{RR}} < X \le d$ will not hold. So, in this case, $P_3 = 0$.

When $P_{th} \ge \frac{\gamma_{th}N_0}{(1-\rho) - \eta\rho\gamma_{th}\Omega_{RR}}$, P_3 can be reformulated as

$$P_3 = \Pr\left\{\frac{\eta\rho P_sXY}{N_0} > \gamma_{th}, \frac{\gamma_{th}N_0}{(1-\rho)P_s - \eta\rho P_s\gamma_{th}\Omega_{RR}} < X \le d\right\}$$
$$= \int_{\chi}^{d} \Pr\left(\frac{\eta\rho P_sxY}{N_0} > \gamma_{th}\right) f_X(x)dx = \lambda_{SR}\int_{\chi}^{d} \exp\left(-\frac{\lambda_{RD}\gamma_{th}N_0}{\eta\rho P_sx}\right)\exp\left(-\lambda_{SR}x\right)dx, \quad (35)$$

where $\chi = \frac{\gamma_{th}N_0}{(1-\rho)P_s - \eta\rho P_s\gamma_{th}\Omega_{RR}}$.

As it is difficult to find the closed-form expression for P_3 due to the integral $\int_{m_1}^{m_2} \exp\left(\frac{v_1}{x}\right) \exp\left(v_2 x\right) dx$ for any value of v_1 and, $v_2 \neq 0$, we will employ the Gaussian–Chebyshev quadrature.

First, we have to change the variable from equation (35) by denoting $x = \frac{d-\chi}{2} y + \frac{d+\chi}{2}$. Equation (35) can be rewritten as

$$\begin{aligned} P_3 &= \frac{\lambda_{SR}(d-\chi)}{2} \int_{-1}^{1} \exp\left[-\frac{\lambda_{RD}\gamma_{th}N_0}{\eta\rho P_s\left(\frac{d-\chi}{2} y + \frac{d+\chi}{2}\right)} \right] \\ &\qquad \exp\left[-\lambda_{SR}\left(\frac{d-\chi}{2} y + \frac{d+\chi}{2}\right) \right] dy \\ &= \frac{\lambda_{SR}(d-\chi)}{2} \times \exp\left[-\frac{\lambda_{SR}(d+\chi)}{2} \right] \times \int_{-1}^{1} \exp\left[-\frac{\lambda_{RD}\gamma_{th}N_0}{\eta\rho P_s G(y)} - \frac{\lambda_{SR}(d-\chi)}{2} y \right] dy , \end{aligned} \tag{36}$$

where $G(y) = \frac{d-\chi}{2} y + \frac{d+\chi}{2}$.

Apply the Gaussian–Chebyshev quadrature from [39–43]. Then equation (36) can be approximated as

$$P_3 \approx \frac{\pi(d-\chi)\lambda_{SR}}{2N} \exp\left[-\frac{\lambda_{SR}(d+\chi)}{2} \right] \sum_{n=1}^{N} \sqrt{1-\mu_n^2} \times \exp\left[-\frac{\lambda_{RD}\gamma_{th}N_0}{\eta\rho P_s G(\theta_n)} - \frac{\lambda_{SR}(d-\chi)}{2} \theta_n \right], \tag{37}$$

where N is a parameter that determines the tradeoff between complexity and accuracy for the Gaussian–Chebyshev quadrature based approximation and $\mu_n = \cos\frac{2n-1}{2N}\pi$ and $\theta_n = \frac{d-\chi}{2}\mu_n + \frac{d-\chi}{2}$.

From equation (33), P_4 is defined as

$$\begin{aligned} P_4 &= \Pr\left\{ \frac{(1-\rho)P_s X}{\eta\rho P_{th}\Omega_{RR} + N_0} > \gamma_{th}, \frac{\eta\rho P_{th} Y}{N_0} > \gamma_{th}, X > d \right\} \\ &= \Pr\left\{ X > \frac{\gamma_{th}(\eta\rho P_{th}\Omega_{RR} + N_0)}{(1-\rho)P_s}, X > d, Y > \frac{\gamma_{th}N_0}{\eta\rho P_{th}} \right\} \\ &= \Pr\{X > \Lambda\} \Pr\left(Y > \frac{\gamma_{th}N_0}{\eta\rho P_{th}} \right) = \exp\left(-\lambda_{SR}\Lambda - \frac{\lambda_{RD}\gamma_{th}N_0}{\eta\rho P_{th}} \right), \end{aligned} \tag{38}$$

where $\Lambda = \max\left[\frac{\gamma_{th}(\eta\rho P_{th}\Omega_{RR} + N_0)}{(1-\rho)P_s}, d \right]$.

Finally, the OP in the DF mode can be claimed from equations (37) and (38) as

$$OP_{DF} \approx 1 - \frac{\pi(d-\chi)\lambda_{SR}}{2N} \exp\left[-\frac{\lambda_{SR}(d+\chi)}{2}\right] \sum_{n=1}^{N} \sqrt{1-\mu_n^2} \times \exp\left[-\frac{\lambda_{RD}\gamma_{th}N_0}{\eta\rho P_s G(\theta_n)} - \frac{\lambda_{SR}(d-\chi)}{2}\theta_n\right] - \exp\left(-\lambda_{SR}\Lambda - \frac{\lambda_{RD}\gamma_{th}N_0}{\eta\rho P_{th}}\right). \quad (39)$$

4. NUMERICAL RESULTS AND DISCUSSION

In this section, we present numerical results to demonstrate the system performance of the system network proposed in the previous section. The correctness of the analytical analysis in the previous section is verified by the Monte Carlo simulation as in [31–35].

In Fig. 3 we depict the OP as a function of ψ using $\eta = 0.8$, $\gamma_{th} = 0.25$ and $\rho = 0.2$ and 0.5. Here we vary ψ from –15 DB to 20 dB for validating the correctness of the proposed system. We can observe in Fig. 3 that the system OP shows a massive decrease with the rising of the ψ from –5 dB to 10 dB. At the beginning and at the last values of the ψ, the system OP has a slight fall. Figure 4 illustrates the system OP versus the P_{th} while the P_{th} increases from 0 dB to 15 dB. In Fig. 4 we set the primary system parameters as $\eta = 0.8$, $\gamma_{th} = 0.25$, $\rho = 0.5$, and ψ = 5 and 10 dB. As shown in Fig. 4, the system OP decreases significantly with the rising of the power P_{th}. It can be observed that the higher the P_{th} in the system, the lower the system OP may become.

From Figs 3 and 4 we can see that the analytical curves and the simulation curves duplicate each other for validating the analytical analysis in the above section. The system OP in case $\rho = 0.2$ with a high SNR in Fig. 3 for the AF and DF modes can reach the value of 0.55, and the system OP with $\rho = 0.5$ with the AF and DF modes can reach the value of 0.3. In the same way, when the power P_{th} rises to higher values, the system OP in the case ψ = 5 can reach the value of 0.4 with the AF mode and 0.2 with the DF mode. However, in the ψ = 10 case, the system OP can obtain the value of 0.2 for the AF mode and 0.1 for the DF mode.

Next, in Fig. 5, we depict the influence of the power splitting factor ρ on the system OP with ψ = 5 dB, $\gamma_{th} = 0.15$, and $\eta = 0.5$ and 0.7. In Fig. 5, ρ increases from 0 to 1, and we considered both AF and DF modes. As shown in Fig. 5, the system OP decreases considerably when ρ rises from 0 to 0.6, and after reaching the optimal value, the system OP shows an immense increase when ρ rises to 1. The optimal value of the system OP can be obtained with ρ from 0.5 to 0.7.

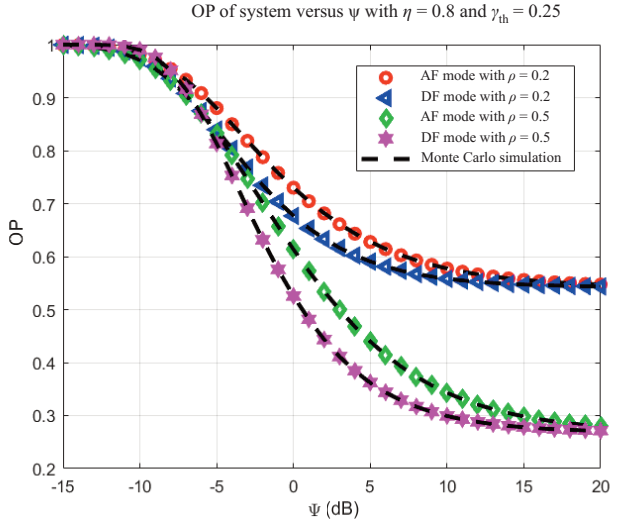

Fig. 3. Outage probability (OP) versus the energy P_s to variance N_0 ratio ψ.

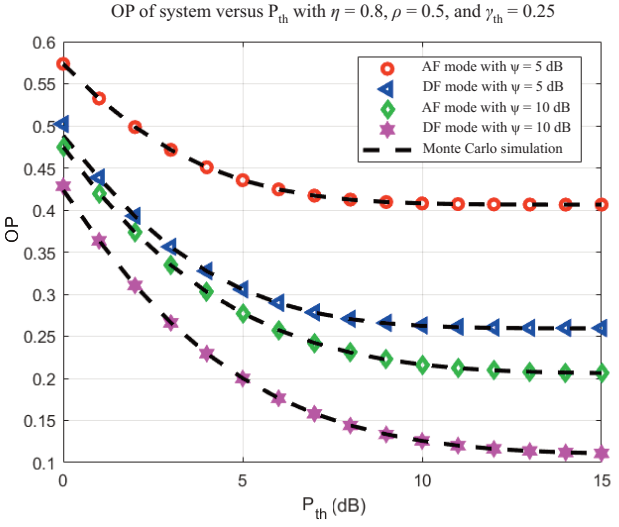

Fig. 4. Outage probability (OP) versus the saturation threshold of the rechargeable power P_{th}.

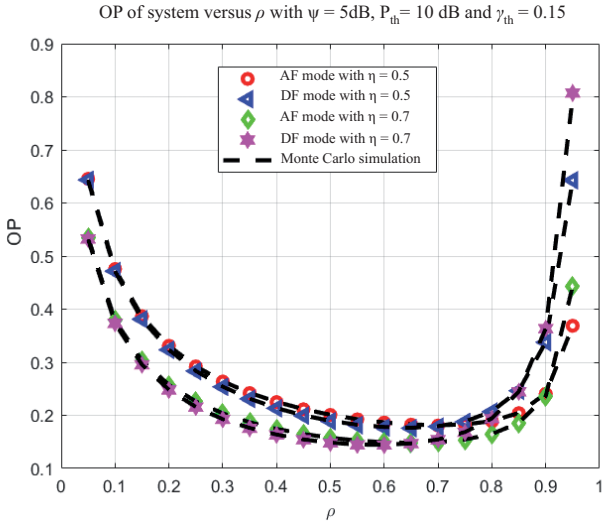

Fig. 5. Outage probability (OP) versus the power-splitting factor ρ.

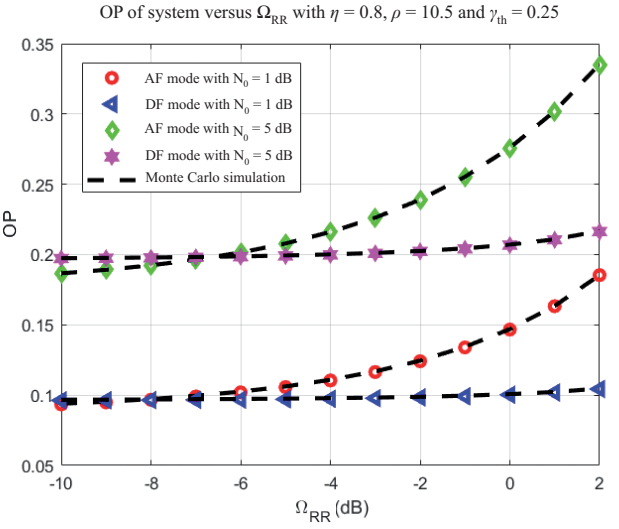

Fig. 6. Outage probability (OP) versus the variance of $|h_{RR}|^2$ Ω_{RR}.

Furthermore, we investigated the system OP as the function of the Ω_{RR} as shown in Fig. 6. In Fig. 6 the Ω_{RR} increases from –10 dB to 2 dB, and the main system parameters are set as $\psi = 5$ dB, $\gamma_{th} = 0.25$, $\eta = 0.8$, $\rho = 0.5$, and $N_0 = 1$ dB and 5 dB. The results demonstrate that with the rising of the Ω_{RR} the system OP of the AF mode increases significantly, but that of the DF mode shows just a slight increase. Consequently, with a rising Ω_{RR} the system performance of the DF mode is better than of the AF mode. Finally, as illustrated in Figs 5 and 6, the simulation results agree well with the analytical results.

Figure 7 examines the impact of the N_0 on the system OP with $\eta = 0.8$, $\gamma_{th} = 0.25$, $\eta = 0.8$, $\rho = 0.25$, and $\Omega_{RR} = 1$ dB and 5 dB. As shown in Fig. 7, the system OP of both AF and DF modes has a considerable increase with the continuous rising of N_0 from –10 dB to 5 dB. This is due to the fact that the more energy is used for the harvesting phase, the higher the OP in the proposed system.

The system OP as the function of the energy efficiency η is illustrated in Fig. 8. Here the energy efficiency η varies from 0 to 1, and the main system parameters are set as $\psi = P_{th} = 5$ dB, $\rho = 0.5$, and $\gamma_{th} = 0.15$ and 0.25. In contrast to Fig. 7, the system OP has a colossal decrease with the rising of the energy efficiency η. This suggests that the more efficient energy use, the lower system OP can be obtained and the better system

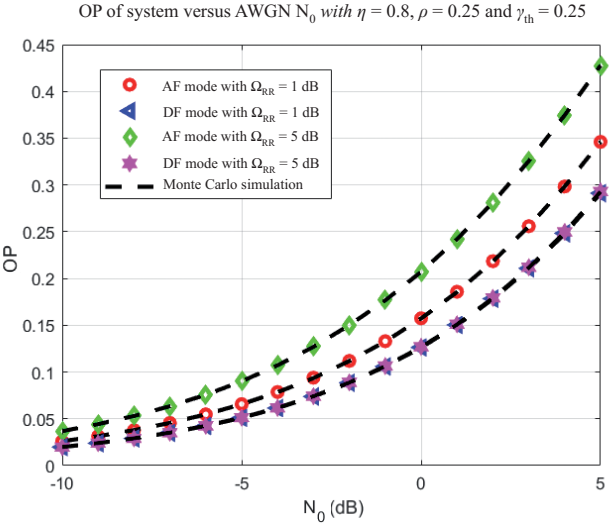

Fig. 7. Outage probability (OP) versus the AWGN variance N_0.

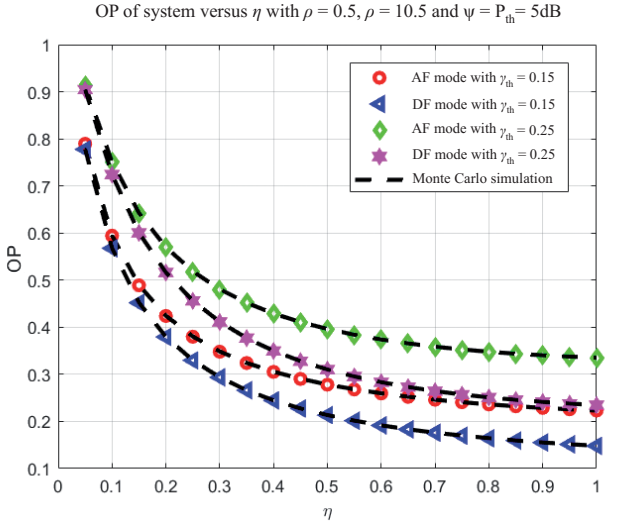

Fig. 8. Ooutage probability (OP) versus the energy conversion efficiency η.

performance is achieved. As shown in Figs 7 and 8, the simulation curves overlap the analytical curves and thus verify the analytical expressions in the previous section.

5. CONCLUSIONS

In this paper, the system performance analysis of NEH based PS relaying in the FD relaying network is proposed and investigated. The closed-form expressions of the system OP are analysed and derived for both AF and DF modes. Then, the correctness of the analytical OP is verified by using the Monte Carlo simulation. Furthermore, the influence of the primary system parameters on the system OP is investigated. The research results showed that the simulation curves and the analytical curves overlapped, verifying the correctness of the analytical expressions. This paper can be considered as a novel recommendation for EH communication relaying networks.

ACKNOWLEDGEMENTS

This research was supported by the Industrial University of Ho Chi Minh City (IUH), Vietnam, under grant No. 72/HD-DHCN and VSB - Technical Univesity of Ostrava, Chech Republic, grant SGS, registration No. SP2020/65. The publication costs of this article were partially covered by the Estonian Academy of Sciences.

REFERENCES

1. Bi, S., Ho, C. K., and Zhang, R. Wireless powered communication: oportunities and challenges. *IEEE Commun. Mag*., 2015, **53**(4), 117–125.
2. Niyato, D., Kim, D. I., Maso, M., and Han, Z. Wireless powered communication networks: research directions and technological approaches. *IEEE Wireless Commun*., 2017, **24**(6), 2–11.
3. Yu, H., Lee, H., and Jeon, H. What is 5G? Emerging 5G mobile services and network requirements. *Sustainability*, 2017, **9**(10), 1848.
4. Salem, A., Hamdi, K. A., and Rabie, K. M. Physical layer security with RF energy harvesting in AF multi-antenna relaying networks. *IEEE Trans. on Commun*., 2016, **64**(7), 3025–3038.
5. Liu, W., Zhou, X., Durrani, S., and Popovski, P. Secure communication with a wireless-powered friendly jammer. *IEEE Trans. Wireless Commun*., 2016, **15**(1), 401–415.
6. Nguyen, B. C., Hoang, T. M., Tran, P. T., and Nguyen,T. N. Outage probability of NOMA system with wireless power transfer at source and full-duplex relay. *AEU-Int. J. Electron. Commun.*, 2020, **116**, March 2020, 152957.
7. Zhou, X., Zhang, R., and Ho, C. K. Wireless information and power transfer: architecture design and rate-energy tradeoff. *IEEE Trans. Commun*., 2013, **61**(11), 4754–4767.
8. Liu, L., Zhang, R., and Chua, K-C. Wireless information transfer with opportunistic energy harvesting. *IEEE Trans. Wireless Commun*., 2013, **12**(1), 288–300.
9. Nguyen, T. N., Tran, M., Ha, D-H., Trang, T. T., and Voznak, M. Multi-source in DF cooperative networks with the PSR protocol based full-duplex energy harvesting over a Rayleigh fading channel: performance analysis. *Proc. Estonian Acad. Sci.*, 2019, **68**, 264–275.
10. Medepally, B. and Mehta, N. B. Voluntary energy harvesting relays and selection in cooperative wireless networks. *IEEE Trans. Wireless Commun*., 2010, **9**(11), 3543–3553.
11. Zhang, R. and Ho, C. K. MIMO broadcasting for simultaneous wireless information and power transfer. In *2011 IEEE Global Telecommunications Conference – GLOBECOM 2011*, 2011. arXiv:1105.4999v3.
12. Son, H. and Clerckx, B. Joint beamforming design for multi-user wireless information and power transfer. *IEEE Trans. Wireless Commun.*, 2014, **13**(11), 6397–6409.
13. Xu, J., Liu, L., and Zhang, R. Multiuser MISO beamforming for simultaneous wireless information and power transfer. *IEEE Trans. Signal Processing*, 2014, **62**(18), 4798–4810.
14. Park, J. and Clerckx, B. Joint wireless information and energy transfer in a two-user MIMO interference channel. *IEEE Trans. Wireless Commun.*, 2013, **12**(8), 4210–4221.
15. Huang, K. and Larsson, E. Simultaneous information and power transfer for broadband wireless systems. *IEEE Trans. Signal Processing*, 2013, **61**(23), 5972–5986.
16. Zhou, X., Zhang, R., and Ho, C. K. Wireless information and power transfer in multiuser OFDM systems. *IEEE Trans. Wireless Commun.*, 2014, **13**(4), 2282–2294.
17. Nasir, A. A., Zhou, X., Durrani, S., and Kennedy, R. A. Relaying protocols for wireless energy harvesting and information processing. *IEEE Trans. Wireless Commun*., 2013, **12**(7), 3622–3636.

18. Huang, Y. and Clerckx, B. Joint wireless information and power transfer for an autonomous multiple antenna relay system. *IEEE Commun. Lett.*, 2015, **19**(7), 1113–1116.
19. Huang, Y. and Clerckx, B. Relaying strategies for wireless-powered MIMO relay networks. *IEEE Trans. Wireless Commun.*, 2016, **15**(9), 6033–6047.
20. Ju, H. and Zhang, R. Throughput maximization in wireless powered communication networks. *IEEE Trans. Wireless Commun.*, 2014, **13**(1), 418–428.
21. Lee, H., Lee, K-J., Kim, H., Clerckx, B., and Lee, I. Resource allocation techniques for wireless powered communication networks with energy storage constraint. *IEEE Trans. Wireless Commun.*, 2016, **15**(4), 2619–2628.
22. Huang, K., Zhong C., and Zhu, G. Some new research trends in wirelessly powered communications. *IEEE Wireless Commun.*, 2016, **23**(2), 19–27.
23. Pflug, H. W., Keyrouz, S., and Visser, H. J. Far-field energy harvesting rectifier analysis. In *2016 IEEE Wireless Power Transfer Conference (WPTC2016)* Aveiro, 2016.
24. Nguyen, T. N., Tran, M. H., Nguyen, T-L., Ha, D-H., and Voznák, M. Performance analysis of a user selection protocol in co-operative networks with power splitting protocol-based energy harvesting over Nakagami-m/Rayleigh channels. *Electronics*, 2019, **8**(4), 448.
25. Halima, N. B. and Boujemaa, H. Exact and approximate symbol error probability of cooperative systems with best relay selection and all participating relaying using Amplify and Forward or Decode and Forward Relaying over Nakagami-m fading channels. *KSII Trans. Internet Inf. Syst.*, 2018, **12**(1), 81–108.
26. Tseng, S.-M., Lee, T-L., Ho, Y-C., and Tseng, D-F. Distributed space-time block codes with embedded adaptive AAF/DAF elements and opportunistic listening for multihop power line communication networks. *Int. J. Commun. Syst.*, 2017, **30**(1), e2950.
27. Li, Y. and Vucetic, B. On the performance of a simple adaptive relaying protocol for wireless relay networks. In *Proceedings of the VTC Spring 2008 – IEEE Vehicular Technology Conference, Singapore, 11–14 May 2008*, 2400–2405.
28. Nguyen, T. N., Tran, P. T., and Voznak, M. Power splitting-based energy-harvesting protocol for wireless powered communication networks with a bidirectional relay. *Int. J. Commun. Syst.*, 2018, **31**(13).
29. Assimonis, S. D., Daskalakis, S., and Bletsas, A. Sensitive and efficient RF harvesting supply for batteryless backscatter sensor networks. *IEEE Trans. Microw. Theory Techn.*, 2016, **64**(4), 1327–1338.
30. Popovic, Z. Far-field low-power wireless powering for unattended sensors. In *2015 IEEE 16th Annual Wireless and Microwave Technology Conference (WAMICON)*. Cocoa Beach, Fl., 2015, 1–4.
31. Nguyen, T. N., Minh, T. H. Q., Tran P. T., and Voznak, M. Adaptive energy harvesting relaying protocol for two-way half duplex system network over Rician fading channels. *Wireless Commun. Mobile Comput*., **2018**, 1–10.
32. Nguyen, T. N., Tin, P. T., Ha, D. H., Voznak, M., Tran, P. T., Tran, M., and Nguyen, T-L. Hybrid TSR–PSR alternate energy harvesting relay network over Rician fading channels: outage probability and SER analysis. *Sensors*, 2018,**18**(11), article No. 3839.
33. Nguyen, T N., Minh, T. H. Q., Ha, D-H., Nguyen, T-L., and Voznak, M. Energy harvesting based two-way full-duplex relaying network over Rician fading environment: performance analysis. *Proc. Estonian Acad. Sci*., 2019, **68**, 111–123.
34. Phan, V-D., Nguyen, T. N., Tran, M., Trang, T. T, Voznak, M., Ha, D-H., and Nguyen, T-L. Power beacon-assisted energy harvesting in a half-duplex communication network under co-channel interference over a Rayleigh fading environment: energy efficiency and outage probability analysis. *Energies*, 2019, **12**(13), 2579.
35. Nguyen, T. N., Minh, T. H. Q., Nguyen, T-L., Ha, D-H., and Voznak, M. Multi-source power splitting energy harvesting relaying network in half-duplex system over block Rayleigh fading channel: system performance analysis. *Electronics*, 2019, **8**(1), article No. 67.
36. Dong, Y., Hossain, M. J., and Cheng, J. Performance of wireless powered amplify and forward relaying over Nakagami-m fading channels with nonlinear energy harvester. *IEEE Commun. Lett*., 2016, **20**(4), 672–675.
37. Wang, K., Li, Y., Ye, Y., and Zhang, H. Dynamic power splitting schemes for non-linear EH relaying networks: perfect and imperfect CSI. In *2017 IEEE 86th Vehicular Technology Conference (VTC-Fall).* Toronto, ON, 2017, 1–5.
38. Gradshteyn, I. S. and Ryzhik, I. M. *Table of Integrals, Series, and Products*, *8th ed*. (Zwillinger, D. ed.). Elsevier, Academic Press, 2014.
39. Nguyen, T. N., Tran, P. T., Minh, T. H. Q., Voznak, M., and Sevcik, L. Two-way half duplex decode and forward relaying network with hardware impairment over Rician fading channel: system performance analysis. *Elektron. Elektrotech.*, 2018, **24**(2), 74–78.
40. Ye, Y., Li, Y., Wang, D., Zhou, F., Hu, R. Q., and Zhang, H. Optimal transmission schemes for DF relaying networks using SWIPT. *IEEE Trans. Vehicular Technol.*, 2018, **67**(8), 7062–7072.
41. Tin, P. T., Hung, D., T, Nguyen, T. N., Duy, T. T., and Voznak, M. Secrecy performance enhancement for underlay cognitive radio networks employing cooperative multi-hop transmission with and without presence of hardware impairments. *Entropy*, 2019, **21**(2), article No. 217.
42. Nguyen, T. N., Tran, M., Tran, P. T., Tin, P. T., Nguyen, T-L., Ha, D-H., and Voznak, M. On the performance of power splitting energy harvested wireless full-duplex relaying network with imperfect CSI over dissimilar channels. *Secur. Commun. Netw.*, **2018**, article ID 6036087.
43. Tin, P. T., Nguyen, T. N., Tran, M., Trang, T. T., and Sevcik, L. Exploiting direct link in two-way half-duplex sensor network over block Rayleigh fading channel: upper bound ergodic capacity and exact SER analysis. *Sensors*, 2020, **20**(4), article No. 1165.